Helical inversions and phase separations in binary mixtures of cholesteric liquid crystalline molecules

doi: info:doi/10.1080/02678292.2018.1468041

Liquid Crystals
Vol. 00, No. 00, Month 200x, 1–20

Articles

Helical inversions and phase separations in binary mixtures of cholesteric liquid crystalline molecules

Akihiko Matsuyama* and Tatsuaki Kan

Department of Bioscience and Bioinformatics, Faculty of Computer Science and Systems Engineering, Kyushu Institute of Technology, Kawazu 680-4, Iizuka, Fukuoka 820-8502, JAPAN

(*Jan. 2018*)

A mean field theory is introduced to describe a helical inversion in nematic-cholesteric mixtures and binary cholesteric mixtures. Taking into account a chiral coupling between unlike molecules, the helical pitch is derived as a function of orientational order parameters and concentration. We find the conditions of helical inversions for the mixtures and derive the concentration of the helical inversions, depending on the chiral interaction. The numerical results are in agreement with the experimental results. We also examine phase separations on the temperature-concentration plane, including the helical inversions. A large variety of phase separations, such as the two-phase coexistence between a right-handed rich and a left-handed rich phase, etc., are predicted.

Keywords: helical inversion; cholesteric; chiral nematic; cholesteric mixture, phase separation

1. Introduction

Chiral mesophases, or chiral nematic phases, in binary mixtures of nematic and cholesteric liquid crystalline (LC) molecules and mixtures of cholesteric LC molecules exhibit helical structures with a pitch and a helix sense. The helical structures in these chiral LC mixtures depend on the concentration and temperature.(*1–4*). Many experimental observations of the helical inversions have been reported.(*5–16*) For example, it is well known that a chiral mixture of a right- and a left-handed chiral LC molecule shows an inversion of the screw sense at a particular concentration.(*5–9*) The mixture of nematic MBBA (*p*-methoxybenzylidene-*p*-*n*-butylaniline) and cholesteric cholesteryl chloride exhibits the helical inversion by changing the concentration.(*10, 18*) In a mixture of two cholesteric molecules with the same helical sense in the pure state, a twofold inversion of the helix has been observed.(*13*) Helical inversions in mixtures of a nematic liquid crystal and nematic-like compounds with asymmetric side chains have also been systematically investigated .(*14, 15*)

Theoretical studies for the helical inversion in binary cholesteric mixtures have been presented by many authors.(*17–30*) Stegemeyer and Finkelmann have studied the helical inversions of the binary cholesteric mixtures by means of the Goossens

*Corresponding author. Email: matuyama@bio.kyutech.ac.jp

ISSN: 0267-8292 print/ISSN 1366-5855 online

DOI: 10.1080/0267829YYxxxxxxxx
http://www.informaworld.com

theory,(*17*) where asymmetric dipole-quadrupole interactions in the twist angle have been taken into account.(*12, 13, 21*) Lin-Liu et. al. have considered a general form for intermolecular interactions of chirality and discussed the behavior of the temperature dependent pitch.(*23, 24*) Varichon et. al. have extended the Lin-Liu theory to lyotropic systems and described helical inversions, but a physical interpretation of the parameters remains difficult. Adams et. al. reported a phenomenological treatment of the dependence of the pitch on concentration.(*19*) The theory has provided a mathematical satisfactory description of the observed dependence of the pitch in the mixtures on concentration, however, orientational order parameters of the components in the chiral mixtures have not been considered. The orientational order parameters are significantly important to study both isotropic(I)-cholesteric(Ch) phase transitions (CIT), or phase separations,(*32–37*) and helical inversions in binary cholesteric mixtures. The importance of molecular biaxiality of chiral molecules has also been recognized by some authors.(*28–31*) Emelyanenko, Osipov, and Dunmur have taken into account the order parameters for the nematic ordering of the long molecular axis and that of the short molecular axis of biaxial molecules in a uniaxial nematic phase and shown that the molecular biaxiality is important in determining the variation of the helical pitch with temperature and concentration.(*28*)

In this paper, we present a molecular theory to describe the CIT and the helical sense in binary mixtures of cholesteric molecules. We here neglect the molecular biaxiality. Based on our recent mean field theories for the Ch phase(*38, 39*) and twist-bend nematic phase(*40, 41*), nematic-cholesteric mixtures and binary cholesteric mixtures are examined. We derive the pitch wavenumber of the helix as a function of orientational order parameters and concentration. The results are consistent with the approximate formulas obtained by Stegemeyer and Finkelmann.(*21*). The helical inversion takes place at a particular concentration, depending on the chiral interaction between unlike components. The conditions of the helical inversions are found in nematic-cholesteric mixtures and binary cholesteric mixtures. Our theory has a good agreement with the experimental results. We also examine phase separations and helical inversions on the temperature-concentration plane. We predict a rich variety of phase separations due to the helical sense: for example, a phase separation between a right-handed rich and a left-handed rich phase, etc..

In the next section, we introduce the free energy for mixtures of cholesteric liquid crystals. In Section 3.1, the numerical results for mixtures of nematic and cholesteric LC molecules are shown. The properties of binary cholesteric mixtures are discussed in Section 3.2. The phase transitions and phase separations accompanied helical inversions are discussed in Section 3.3.

2. Free energy of a binary mixture of LC molecules with chiral interactions

In this section, we introduce the free energy of a binary mixture of cholesteric LC molecules with chiral interactions.

Consider a binary mixture of LC molecules A and B. Let N_A be the number of the LC molecule A of the length L_A with diameter D and N_B be the number of the LC molecule B of the length L_B with diameter D. We define the axial ratio $n_i \equiv L_i/D$. The volume of the LC molecule A and that of B are given by $v_A = a^3 n_A$ and $v_B = a^3 n_B$, respectively, where we define $a^3 \equiv (\pi/4)D^3 \simeq D^3$. Let $\phi_A = v_A N_A/V$ and $\phi_B = v_B N_B/V$ be the volume fraction of the molecule A and B, respectively, where V is the volume of the system: $\phi_A + \phi_B = 1$.

The free energy of the mixtures consists of the following two terms:

$$F = F_{mix} + F_{ani}. \tag{1}$$

The first term in Equation (1) is the free energy of mixing for the binary mixture and can be given by Flory-Huggins theory for polymer blends:(*42, 43*)

$$f_{mix} \equiv a^3 \beta F_{mix}/V = \frac{\phi_A}{n_A} \ln \phi_A + \frac{\phi_B}{n_B} \ln \phi_B + \chi \phi_A \phi_B, \tag{2}$$

where $\beta \equiv 1/k_B T$; T is the absolute temperature, k_B is the Boltzmann constant and $\chi (\equiv U_0/k_B T)$ is the Flory-Huggins interaction parameter between LC molecules in an isotropic state. The interaction energy U_0 controls the miscibility of the two components. In the case of binary mixtures with a good solubility, we can take $\chi = 0$. For larger values of χ, phase separations take place depending on temperature and concentration.(*32, 33, 43*)

The second term in Equation (1) shows the anisotropic free energy for liquid crystalline ordering. The configuration of a constituent molecule is characterized by its position vector $\mathbf{r}$ and its orientation unit vector $\mathbf{\Omega} = (\sin\theta\cos\varphi, \sin\theta\sin\varphi, \cos\theta)$, defined by a polar angle θ and an azimuthal angle φ, or solid angle $d\Omega (= \sin\theta d\theta d\varphi)$, in a fixed coordinate frame. Let $f_i(\mathbf{n}(\mathbf{r}) \cdot \mathbf{\Omega})$ be the orientational distribution function of the constituent molecule $i (= A, B)$, where $\mathbf{n}(\mathbf{r})$ is the local director. It should be noted that the distribution function depends only on the relative angle between the local director $\mathbf{n}(\mathbf{r})$ and the molecular orientation vector $\mathbf{\Omega}$. The anisotropic part of the free energy in the second virial approximation can be given by(*43, 44*)

$$\begin{aligned} \beta F_{ani} = & \sum_{i=A,B} \rho_i \int f_i(\mathbf{n}(\mathbf{r}) \cdot \mathbf{\Omega}) \ln 4\pi f_i(\mathbf{n}(\mathbf{r}) \cdot \mathbf{\Omega}) d\mathbf{r} d\Omega \\ & + \frac{1}{2} \sum_{i,j=A,B} \rho_i \rho_j \int f_i(\mathbf{n}(\mathbf{r}_1) \cdot \mathbf{\Omega}_1) f_j(\mathbf{n}(\mathbf{r}_2) \cdot \mathbf{\Omega}_2) \\ & \times \beta U_{ij}(\mathbf{r}_1, \mathbf{\Omega}_1; \mathbf{r}_2, \mathbf{\Omega}_2) d\mathbf{R}, \end{aligned} \tag{3}$$

where $d\mathbf{R} \equiv d\mathbf{r}_1 d\mathbf{r}_2 d\Omega_1 \Omega_2$, $\rho_i = N_i/V$ is the number density of the LC molecule i. The first term in Equation (3) shows the entropy changes due to orientational ordering and U_{ij} is the orientation-dependent intermolecular potential between two particles i and j $(i, j = A, B)$. The lowest-order contributions to the interaction potential are given in a series of the Legendre polynomials:(*24, 38–41*)

$$\begin{aligned} U_{ij}(\mathbf{r}_1, \mathbf{\Omega}_1; \mathbf{r}_2, \mathbf{\Omega}_2) = & U_{ij,1}(\mathbf{r}_{12})(\mathbf{\Omega}_1 \times \mathbf{\Omega}_2 \cdot \hat{\mathbf{r}}_{12}) P_1(\mathbf{\Omega}_1 \cdot \mathbf{\Omega}_2) \\ & + U_{ij,2}(\mathbf{r}_{12}) P_2(\mathbf{\Omega}_1 \cdot \mathbf{\Omega}_2), \end{aligned} \tag{4}$$

where $\mathbf{r}_{12} = \mathbf{r}_2 - \mathbf{r}_1$ and $\hat{\mathbf{r}}_{12} (= \mathbf{r}_{12}/|\mathbf{r}_{12}|)$ is a unit vector. The potential $U_{ij,1}$ shows the chiral interaction between LC molecules and the pseudoscalar term $\mathbf{\Omega}_1 \times \mathbf{\Omega}_2 \cdot \hat{\mathbf{r}}_{12}$ represents scalars coupling between orientational and spatial variables. The potential $U_{ij,2}$ shows the intermolecular potential for a nematic phase, which has been used in Onsager(*44*) and Maier-Saupe models.(*45*) As usual we here employ a simple square well interaction potential with a short range $d_0 (\simeq D)$ on the order of the molecule.(*38*) We then define a numerical parameter $c_{ij} \equiv -U_{ij,1}/k_B T$ for a chiral pseudoscalar interaction parameter between LC molecules and $\nu_{ij} \equiv -U_{ij,2}/k_B T (>$

0) for a nematic interaction (or Maier-Saupe) parameter. The interaction parameter $\nu_{ij} > 0$ corresponds to the orientation-dependent (Maier-Saupe) interaction parameter between the LC molecules i and j. The larger values of ν_{ij} imply that the two molecules i and j prefer to be parallel to each other and a nematic phase tends to be more stable in the mixture. The chiral interaction parameter c_{ij} corresponds to the strength of the chirality between the LC molecules i and j. The larger values of c_{ij} show stronger chirality (or twist interaction) between the LC molecules i and j and a twist distortion, or a Ch phase, tends to be more stable in the mixture.

Using the tensor order parameter of the LC molecule $i(= A, B)$:(*33*)

$$\mathcal{Q}^{(i)}_{\alpha\beta}(\mathbf{r}) = S_i\left(\frac{3}{2}n_\alpha(\mathbf{r})n_\beta(\mathbf{r}) - \frac{1}{2}\delta_{\alpha\beta}\right), \tag{5}$$

where $\delta_{\alpha\beta}$ is the Kronecker delta function, n_α is the $\alpha(= x, y, z)$ component of the director $\mathbf{n}$, and S_i is the scalar orientational order parameter of the molecule i:

$$S_i = \int P_2(\mathbf{n}(\mathbf{r})\cdot\mathbf{\Omega}) f_i(\mathbf{n}(\mathbf{r})\cdot\mathbf{\Omega}) d\Omega, \tag{6}$$

the anisotropic free energy (Equation (3)) is given by(*40, 41*)

$$\begin{aligned} a^3\beta F_{ani}/V = &\sum_{i=A,B}\frac{\phi_i}{n_i}\int f_i(\mathbf{n}(\mathbf{r})\cdot\mathbf{\Omega})\ln 4\pi f_i(\mathbf{n}(\mathbf{r})\cdot\mathbf{\Omega})d\Omega \\ &+\sum_{i,j=A,B}\Bigg[-\frac{1}{2}\nu_{ij}\phi_i\phi_j\frac{2}{3}\mathcal{Q}^{(i)}_{\alpha\beta}(\mathbf{r})\mathcal{Q}^{(j)}_{\alpha\beta}(\mathbf{r}) \\ &+\frac{1}{2}\nu_{ij}\phi_i\phi_j\frac{1}{9}\partial_\mu\mathcal{Q}^{(i)}_{\alpha\beta}(\mathbf{r})\partial_\mu\mathcal{Q}^{(j)}_{\alpha\beta}(\mathbf{r})d_0^2 \\ &-\frac{1}{2}c_{ij}\phi_i\phi_j\frac{4}{9}\epsilon_{\alpha\beta\gamma}\mathcal{Q}^{(i)}_{\mu\beta}(\mathbf{r})\partial_\alpha\mathcal{Q}^{(j)}_{\mu\gamma}(\mathbf{r})d_0\Bigg]. \end{aligned} \tag{7}$$

where $\epsilon_{\alpha\beta\gamma}$ is Levi-Civita antisymmetric tensor of the third rank, and $\partial_\mu = \partial/\partial\mu$ is the first spatial derivative of the tensor order parameter $(\alpha, \mu = x, y, z)$.

In order to calculate the distortion free energy of the Ch phase, we assume that the director is uniformly twisted along the z axis with a pitch length $p = 2\pi/q$:

$$\mathbf{n}(\mathbf{r}) = (\cos qz, \sin qz, 0), \tag{8}$$

where q is a wavenumber and the twist angle is $\omega = qz$. When $q > 0$, we have a right-handed helix and a left-handed helix is given by $q < 0$. When $q = 0$, the director is uniformly along the x axis and the mixture shows a nematic phase, where the pitch length diverges. On the other words, the definition of the right-handed helix is given by $\mathbf{e}_x \times \mathbf{n} = (\sin qz)\mathbf{e}_z$ with $q > 0$, where $\mathbf{e}_\alpha$ is a unit vector along the $\alpha(= x, y, z)$ axis. When $q < 0$, we have a left-handed helix.

Substituting Equations (5) and (8) into Equation (7), we obtain the free energy of LC phases:(*38*)

$$F_{ani} = F_{nem} + F_{dis}, \tag{9}$$

where we have separated the anisotropic free energy into two parts. One is the

nematic free energy of Maier-Saupe type(*45*):

$$f_{nem} \equiv a^3 \beta F_{nem}/V = \sum_{i=A,B} \frac{\phi_i}{n_i} \int f_i(\mathbf{n}(\mathbf{r}) \cdot \mathbf{\Omega}) \ln 4\pi f_i(\mathbf{n}(\mathbf{r}) \cdot \mathbf{\Omega}) d\Omega$$
$$-\frac{1}{2}\nu_A \phi_A^2 S_A^2 - \nu_{AB}\phi_A\phi_B S_A S_B$$
$$-\frac{1}{2}\nu_B \phi_B^2 S_B^2, \tag{10}$$

where we write $\nu_A \equiv \nu_{AA}$ and $\nu_B \equiv \nu_{BB}$ for simplicity. The other is the distortion free energy due to the spatial variation of the director for a Ch phase, or a chiral nematic N^* phase:

$$f_{dis} \equiv a^3 \beta F_{dis}/V = \frac{1}{2}\nu_A \phi_A^2 S_A^2 g_A(Q) + \nu_{AB}\phi_A\phi_B S_A S_B g_{AB}(Q)$$
$$+\frac{1}{2}\nu_B \phi_B^2 S_B^2 g_B(Q), \tag{11}$$

where we define the functions g_i as a function of the pitch wavenumber $Q \equiv qd_0$:

$$g_A(Q) \equiv \frac{1}{2}Q(Q - 2Q_A), \tag{12}$$

$$g_{AB}(Q) \equiv \frac{1}{2}Q(Q - 2Q_{AB}), \tag{13}$$

and

$$g_B(Q) \equiv \frac{1}{2}Q(Q - 2Q_B), \tag{14}$$

with $Q_A \equiv c_A/\nu_A$, $Q_B \equiv c_B/\nu_B$ and $Q_{AB} \equiv c_{AB}/\nu_{AB}$ (Note that the notations Q_A and Q_{AB} have been described as Q_0 and α_x in the previous paper, respectively (*38*)). When $\phi_i = 1$ ($i = A$ or B), the function g_i has a minimum at $Q = Q_i$. Apparently, the value of Q_i corresponds to the dimensionless wavenumber of the N^* phase in the pure LC molecule i and is given by $Q_i (\equiv c_i/\nu_i) = 2\pi d_0/p_i$, where p_i is the pitch length of the pure component i. When $Q = 0$ (or a nematic phase), we have $f_{dis} = 0$.

2.1. *Distribution functions in an equilibrium state*

The orientational distribution function $f_A(\mathbf{n}(\mathbf{r}) \cdot \mathbf{\Omega})$ of the LC molecule A and $f_B(\mathbf{n}(\mathbf{r}) \cdot \mathbf{\Omega})$ of the component B are determined by the free energy (Equation (9)) with respect to these functions: $(\delta F_{LC}/\delta f_i) = 0$, under the normalization condition:

$$\int f_i(\mathbf{n}(\mathbf{r}) \cdot \mathbf{\Omega}) d\Omega = 1. \tag{15}$$

We then obtain

$$f_A(x) = \frac{1}{Z_A} \exp\left[\Gamma_A P_2(x)\right], \tag{16}$$

and

$$f_B(x) = \frac{1}{Z_B} \exp\left[\Gamma_B P_2(x)\right], \tag{17}$$

where we define

$$\Gamma_A \equiv n_A \Big[\nu_A \phi_A S_A \big(1 - g_A(Q)\big) + \nu_{AB} \phi_B S_B \big(1 - g_{AB}(Q)\big)\Big], \tag{18}$$

and

$$\Gamma_B \equiv n_B \Big[\nu_B \phi_B S_B \big(1 - g_B(Q)\big) + \nu_{AB} \phi_A S_A \big(1 - g_{AB}(Q)\big)\Big]. \tag{19}$$

The constants Z_A and Z_B are determined by the normalization condition (Equation (15)) as $Z_A = 4\pi I_0(S_A, S_B)$ and $Z_B = 4\pi J_0(S_A, S_B)$, respectively. The functions I_m and J_m are defined as:

$$I_m(S_A, S_B) \equiv \int_0^1 [P_2(x)]^m \exp\left[\Gamma_A P_2(x)\right] dx, \tag{20}$$

$$J_m(S_A, S_B) \equiv \int_0^1 [P_2(x)]^m \exp\left[\Gamma_B P_2(x)\right] dx, \tag{21}$$

respectively, where $m = 0, 1, 2 \cdots$.

Substituting Equations (16) and (17) into (6), the scalar orientational order parameters S_A and S_B can be determined by the two coupled-self-consistent equations:

$$S_A = I_1(S_A, S_B)/I_0(S_A, S_B), \tag{22}$$

and

$$S_B = J_1(S_A, S_B)/J_0(S_A, S_B). \tag{23}$$

Using the distribution functions (16) and (17), the free energy (Equation (9)) of the LC phases is given by

$$\begin{aligned} a^3 \beta F_{ani}/V = & \frac{1}{2}\nu_A \phi_A^2 S_A^2 \big(1 - g_A(Q)\big) \\ & + \nu_{AB} \phi_A \phi_B S_A S_B \big(1 - g_{AB}(Q)\big) \\ & + \frac{1}{2}\nu_B \phi_B^2 S_B^2 \big(1 - g_B(Q)\big) \\ & - \frac{\phi_A}{n_A} \ln I_0 - \frac{\phi_B}{n_B} \ln J_0. \end{aligned} \tag{24}$$

When $Q = 0$, Equation (24) results in the nematic free energy of a binary mixture of LC molecules.(*32, 46*) The total free energy (F) is given by the sum of Equations (2) and (24) .

2.2. *Determination of the pitch length*

We here derive the equilibrium pitch wavenumber $Q^*(\equiv 2\pi d_0/p)$ in a thermal equilibrium state. The procedure is to minimize the distortion free energy f_{dis} (Equation (11)), with respect to Q: $(\partial f_{dis}/\partial Q)_{S_i} = 0$. It is convenient to rewrite the distortion free energy f_{dis} as follows:

$$f_{dis} = \frac{1}{2}\nu_A\big(\phi_A^2 S_A^2 + 2\epsilon_n \phi_A\phi_B S_A S_B + \epsilon_{nB}\phi_B^2 S_B^2\big)g(Q), \tag{25}$$

where we define the numerical parameters: $\epsilon_n \equiv \nu_{AB}/\nu_A$ and $\epsilon_{nB} \equiv \nu_B/\nu_A$, and the distortion function is given by

$$g(Q) \equiv Q(\frac{1}{2}Q - Q^*). \tag{26}$$

Then, the equilibrium pitch wavenumber is given by

$$\begin{aligned} Q^* &\equiv \frac{c_A\phi_A^2 S_A^2 + 2c_{AB}\phi_A\phi_B S_A S_B + c_B\phi_B^2 S_B^2}{\nu_A\phi_A^2 S_A^2 + 2\nu_{AB}\phi_A\phi_B S_A S_B + \nu_B\phi_B^2 S_B^2}, \\ &= \frac{Q_A\phi_A^2 + 2\lambda_x\phi_A\phi_B\tilde{S} + Q_B\epsilon_{nB}\phi_B^2\tilde{S}^2}{\phi_A^2 + 2\epsilon_n\phi_A\phi_B\tilde{S} + \epsilon_{nB}\phi_B^2\tilde{S}^2}, \end{aligned} \tag{27}$$

where we define $\tilde{S} \equiv S_B/S_A$ and the chiral interaction parameter $\lambda_x \equiv c_{AB}/\nu_A$ between unlike components. When $\phi_A = 1$, we obtain $Q^* = c_A/\nu_A = Q_A$. When $\phi_B = 1$, $Q^* = c_B/\nu_B = Q_B$. The wavenumber Q^* and the order parameter $\tilde{S}$ of the mixtures depend on the concentration and temperature.

The twist elastic constant K_{22} of the twist distortion, $(\mathbf{n}\cdot\nabla\times\mathbf{n})^2$ is given by(*38, 40*)

$$aK_{22}/k_BT = \frac{1}{2}\big(\nu_A\phi_A^2 S_A^2 + 2\nu_{AB}\phi_A\phi_B S_A S_B + \nu_B\phi_B^2 S_B^2\big). \tag{28}$$

Then the wavenumber, or a helical twisting power $H_{TP} = Q^*/\phi_A$, is inversely proportional to K_{22}.(*33, 38*)

3. Numerical Results and Discussion

In this section we show the numerical results for the helical pitch of nematic-cholesteric mixtures (Section 3.1) and binary mixtures of cholesteric molecules (Section 3.2). In Section 3.3, we examine the CIT and helical inversions. In the numerical calculations, the reduced-temperature is defined as

$$\tau \equiv T/T_{CI} = 4.5/(n_A\nu_A), \tag{29}$$

where T_{CI} is the CIT temperature of the LC molecule A. Then the numerical parameters are given as a function of the temperature τ: $\nu_A = 4.5/(n_A\tau)$, $\nu_{AB} = \epsilon_n\nu_A$, $\nu_B = \epsilon_{nB}\nu_A$, $c_A = Q_A\nu_A$, $c_{AB} = \lambda_x\nu_A$, $c_B = Q_B\epsilon_{nB}\nu_A$, and $Q_{AB} = \lambda_x/\epsilon_n$.

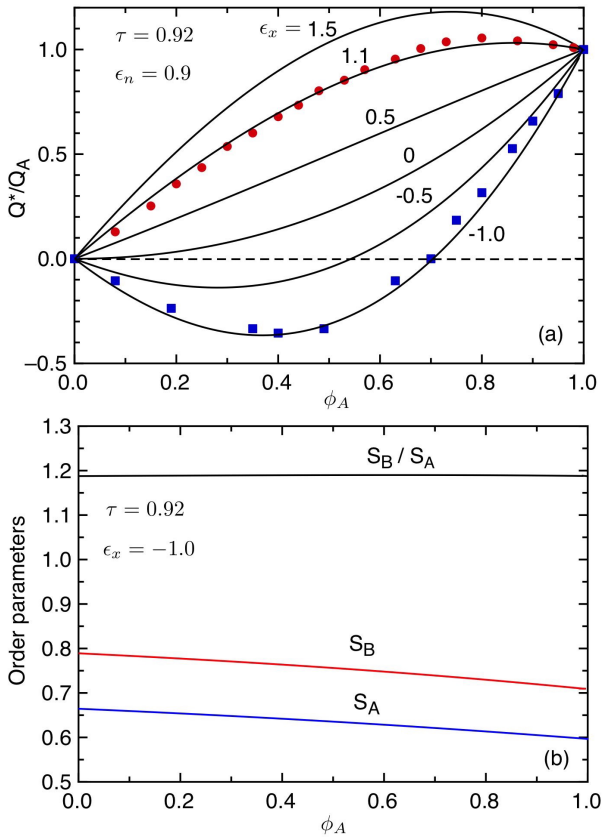

Figure 1. (a) Pitch wavenumber $Q^*/Q_A(= p_A/p)$ plotted against the concentration ϕ_A for various values of $\epsilon_x(= \lambda_x/Q_A)$ at $\tau = 0.92$. The closed circles show the pitch wavenumber observed in the nematic-cholesteric mixture consisting of the nematic MBA and the cholesteric cholesteryl propionate.(*11*) The closed squares show the experimental results in the mixture of the nematic EBBA and cholesteric cholesteryl chloride(*18*). (b) Orientational order parameters S_A, S_B of the Ch phase and the ratio $\hat{S}(= S_B/S_A)$ plotted against the concentration (ϕ_A) of chiral molecules.

3.1. *Helical inversions in mixtures of a nematic and a cholesteric liquid crystalline molecule.*

In this subsection, we examine the helical pitch in mixtures of nematic (component B) and cholesteric (component A) LC molecules. In this case the molecule B has no chirality and then we can take $c_B = 0$, or $Q_B = 0$. The pitch wavenumber Q_A of the pure cholesteric LC molecule A can be estimated as $Q_A = 2\pi d_0/p_A = 0.01$ with a right-handed helix for the typical pitch length $p_A = 300$ nm and the diameter $d_0 = 0.5$ nm of the LC molecule. We here set $n_A = 2$, $n_B = 3$, $\epsilon_n = 0.9$, and $\epsilon_{nB} = 0.9$.

When $Q_A \neq 0$, it is convenient to take $\lambda_x = \epsilon_x Q_A$, where the chiral interaction parameter between unlike molecules is defined as $\epsilon_x \equiv c_{AB}/c_A$. The positive (negative) values of the chiral parameter ϵ_x mean that the chiral interaction (c_{AB}) between the LC molecules A and B favors to twist in the right- (left-) handed direction.

Figure 1(a) shows the equilibrium pitch wavenumber $Q^*/Q_A(= p_A/p)$ plotted against the concentration ϕ_A for various values of ϵ_x at $\tau = 0.92$. When $\epsilon_x < 0$, the chiral interaction between the unlike molecules tends to be a left-handed helix and then the mixture of the nematic LC molecules with small amounts of the chiral molecules A shows a Ch phase with a left-handed helical structure. With increasing the concentration of the chiral dopants ϕ_A, the wavenumber has a minimum and becomes zero at $\phi_A = 0.7$ for $\epsilon_x = -1.0$. This means that the mixture of nematic

and cholesteric molecules becomes a nematic phase at this concentration. Further increasing ϕ_A, a right-handed helix appears. These inversions of the helical pitch have been experimentally observed in nematic-cholesteric mixtures.(*14, 15, 18*) The closed squares show the experimental results of the wavenumber in the mixture of the nematic EBBA and cholesteric cholesteryl chloride.(*18*) When $\epsilon_x = 0 \sim 1$, the wavenumber increases with increasing ϕ_A and there is no helical inversions. For larger values of $\epsilon_x > 1$, the wavenumber has a maximum at a particular concentration and the peak position shifts to lower concentrations and higher wavenumber. These maxima have been observed experimentally.(*11, 14*) The closed circles show the pitch wavenumber observed in the mixture of the nematic MBA and the cholesteric cholesteryl propionate.(*11*) Our theory has a good agreement with the experimental results.

Figure 1(b) shows the orientational order parameters S_A, S_B and the ratio $\tilde{S}(\equiv S_B/S_A)$ plotted against the concentration (ϕ_A) of chiral dopants. The value of $\hat{S}$ is almost constant ~ 1.19 for all concentrations. The values of the order parameters almost do not depend on the chiral interaction ϵ_x. The contribution of the distortion free energy f_{dis}(Equation (11)) to the free energy (Equation (1)) is very small because the distortion function $g(Q^*)$ (Equation (25)) is order of $Q^2 \sim 10^{-4}$ compared to the nematic free energy f_{nem}. Then the orientational order parameters are mainly determined by the nematic free energy f_{nem} (Equation (10)). The value of ϵ_x only affects the pitch wavenumber. That means the denominator of Equation (27) does not depend on ϵ_x and is approximately given by $\sim (\phi_A + \phi_B)^2 = 1$ because of $\epsilon_n \simeq \epsilon_{nB} \sim 1$ and $\tilde{S} \sim 1$. Then the pitch wavenumber (Equation (27)) is given by

$$\begin{aligned} Q^* &\simeq 2\lambda_x \hat{S}\phi_A + (Q_A - 2\lambda_x \hat{S})\phi_A^2 \\ &= Q_A\left[2\epsilon_x \tilde{S}\phi_A + (1 - 2\epsilon_x \tilde{S})\phi_A^2\right]. \end{aligned} \tag{30}$$

At low concentrations of the chiral component (A), the pitch wavenumber is given by the linear-term of ϕ_A and the chiral interaction ϵ_x between unlike components determines the initial slope of the wavenumber as a function of ϕ_A. The dimensionless helical twisting power $H_{NC}(\equiv Q^*/\phi_A)$ at dilute solutions of chiral molecules is given by

$$H_{NC} = 2\lambda_x \tilde{S} = 2Q_A \epsilon_x \tilde{S}. \tag{31}$$

As increasing the concentration of the chiral components, the second term in Equation (30) becomes dominant and the sign of the coefficient of ϕ_A^2 depends on the value of ϵ_x. For larger values of $\epsilon_x > 0$, the second term becomes a negative value and for larger negative values $\epsilon_x < 0$, the second term becomes a positive, as shown in Figure 1(a).

The helical inversion $Q^* = 0$ takes place at

$$\begin{aligned} \phi_{HI} &= 2\lambda_x \tilde{S}/(2\lambda_x \tilde{S} - Q_A) \\ &= 2\epsilon_x \tilde{S}/(2\epsilon_x \tilde{S} - 1). \end{aligned} \tag{32}$$

Then, the condition of the helical inversion is given by

$$\epsilon_x \tilde{S} < 0. \tag{33}$$

Using $\tilde{S} \simeq 1.19$ and $\epsilon_x = -1.0$ in Figure 1(a), we obtain $\phi_{HI} \simeq 0.7$, which is consistent with the numerical result and the experiment (see closed squares on

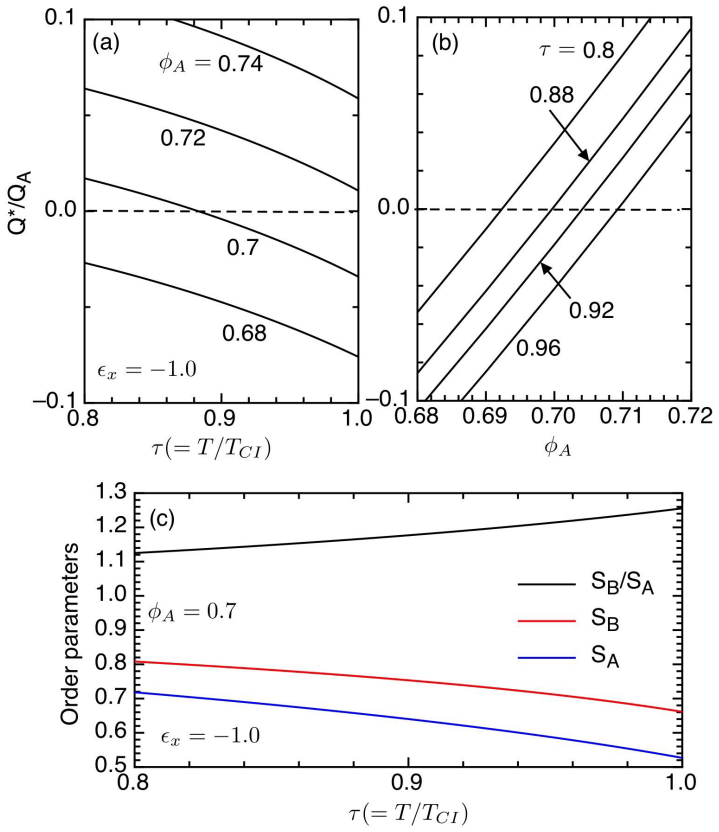

Figure 2. (a) Pitch wavenumber $Q^*/Q_A = p_A/p$ plotted against the temperature τ for various values of the concentration ϕ_A for $\epsilon_x = -1.0$ in Figure 1(a). (b) Pitch wavenumber $Q^*/Q_A = p_A/p$ plotted against the concentration ϕ_A for various values of the temperature τ for $\epsilon_x = -1.0$ in Figure 1(a). (c) Order parameters plotted against the temperature τ for $\phi_A = 0.7$ and $\epsilon_x = -1.0$ in Figure 1(a).

Figure 1(a)). The maximum or minimum of the wavenumber Q^* occurs at

$$\begin{aligned}\phi_m &= \lambda_x \tilde{S}/(2\lambda_x \tilde{S} - Q_A) \\ &= \epsilon_x \tilde{S}/(2\epsilon_x \tilde{S} - 1).\end{aligned} \tag{34}$$

When $\tilde{S} \simeq 1.19$ and $\epsilon_x = 1.1$ (see closed circles on Figure 1(a)), we get the maximum value of Q^* at $\phi_m \simeq 0.8$. When $\tilde{S} \simeq 1.19$ and $\epsilon_x = -1.0$ (see closed squares in Figure 1(a)), we obtain $\phi_m \simeq 0.35$. If the mixture has a helical inversion, the pitch wavenumber has a minimum or a maximum as a function of the concentration of the cholesterics. Equations (32) and (34) have also been obtained by the previous theoretical studies of Stegemeyer and Finkelmann(*21*), where they do not take into account the orientational order parameters. Using Equations (32) and (34), we have $\phi_{HI} = 2\phi_m$, which is consistent with the previous theory.(*21*)

The temperature dependence of the wavenumber Q^* comes from $d\tilde{S}/dT$. As shown in Equation (30), the wavenumber Q^* is a linear function of $\tilde{S}$ and then the value of Q^*/Q_A decreases with increasing temperature when $\epsilon_x > 0$ and $d\tilde{S}/dT < 0$ or $\epsilon_x < 0$ and $d\tilde{S}/dT > 0$. Figure 2(a) shows the pitch wavenumber $Q^*/Q_A = p_A/p$ (Equation (27)) plotted against the temperature τ for various values of the concentration ϕ_A with $\epsilon_x = -1.0$ in Figure 1(a). The pitch wavenumber Q^* decreases with increasing the temperature and the helical inversion takes place at $\tau \simeq 0.88$ for $\phi_A = 0.7$. Figure 2(b) shows the pitch wavenumber Q^*/Q_A plotted against the concentration ϕ_A for various temperatures τ with $\epsilon_x = -1.0$. As increasing temperature, the concentration ϕ_{HI} of the helical inversion increases. Figure 2(c)

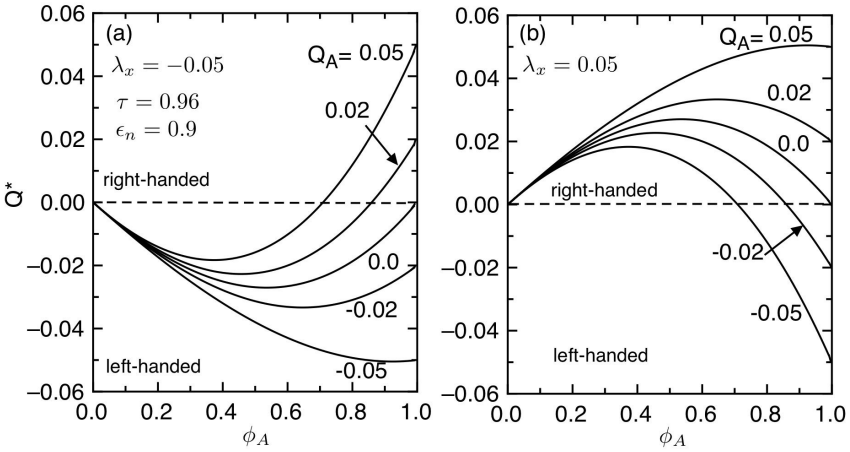

Figure 3. Pitch wavenumber $Q^*(\equiv 2\pi d_0/p)$ plotted against the concentration ϕ_A for various values of the pitch wavenumber Q_A of the pure cholesteric molecule A at $\tau = 0.96$ with the chiral interaction $\lambda_x(\equiv c_{AB}/\nu_A) = -0.05$ (a) and 0.05 (b).

shows the order parameters plotted against the temperature τ for $\phi_A = 0.7$ and $\epsilon_x = -1.0$ in Figure 1(a). The value of the order parameter $\tilde{S}$ is almost $\tilde{S} \sim 1$ and slightly increases with increasing temperature: $d\tilde{S}/dT > 0$, and then we have $dQ^*/dT < 0$ for a negative value of ϵ_x.

In Figure 1, we have examined helical inversions in mixtures of a nematic and a chiral molecule of a right-handed helix. In Figure 3, we discuss the mixtures of nematic and chiral molecules with various handedness Q_A of the pure chiral molecule. Figure 3 shows the pitch wavenumber $Q^*(\equiv 2\pi d_0/p)$ plotted against the concentration ϕ_A for various values of the pitch wavenumber Q_A with $\lambda_x(\equiv c_{AB}/\nu_A) = -0.05$ (a) and 0.05 (b) in Equation (27). When $\lambda_x < 0$ (see Figure 3(a)), where the unlike LC molecules A and B tend to twist in a left-handed helix, the wavenumber Q^* linearly decreases with increasing ϕ_A for large negative values of Q_A. The mixture shows the left-handed helix. As increasing the value of Q_A, the pitch wavenumber Q^* has a minimum at ϕ_{max} and the helical inversion takes place at ϕ_{HI}. Even if $Q_A = 0$, the mixture has a left-handed helix due to the chiral interaction λ_x, or c_{AB}. These behaviors have been experimentally observed(*1, 14*): for example, mixtures of the nematic molecule BBBA (*N*-*p*-butoxybenzylidene-*p*-*n*-butylaniline) and various cholesterics (CN_xCC_{1-x}),(*14*) and mixtures of the nematic PAA (*p*-azoxyanisole) and cholesteric cholesteryl chloride. Using Equation (34), we have $\phi_m = 0.5$ for $Q_A = 0$, which is consistent with the experimental results of the mixture of BBBA and CN_xCC_{1-x} molecules.(*14*) As increasing Q_A, the value of ϕ_m decreases. When $\lambda_x > 0$ (see Figure 3(b)), where the unlike LC molecules A and B favor to twist in the right-handed helix, the pitch wavenumber increases with increasing ϕ_A for large positive values of Q_A. The mixture shows the right-handed helix, where the chiral interaction λ_x dominates. At high concentrations, however, the chirality Q_A of the pure component A, or the second-term in Equation (30), becomes dominant and the helical inversion takes place for $Q_A < 0$. The concentrations ϕ_{HI} and ϕ_m are given by Equations (32) and (34).

Our theory demonstrates that the helical inversions and a maximum or a minimum in the pitch wavenumber Q^* can be understand by using the chiral interaction λ_x between unlike components. When the values of $\lambda_x/Q_A(= \epsilon_x) < 0$, or $c_A c_{AB} < 0$, we have a helical inversion at ϕ_{HI}. The condition of the helical inversion in mixtures of a nematic and a cholesteric molecule is given by $\epsilon_x \tilde{S} < 0$. We also have the relation $\phi_{HI} = 2\phi_m$, that means the value of ϕ_m must be less than 0.5.

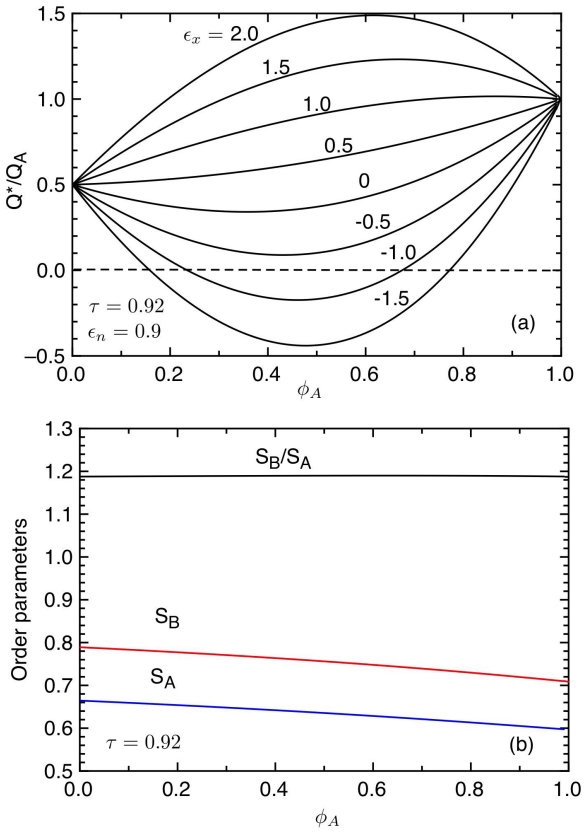

Figure 4. (a) Pitch wavenumber Q^*/Q_A plotted against the concentration ϕ_A for various values of $\epsilon_x (= \lambda_x/Q_A)$ at $\tau = 0.92$ in the binary cholesteric mixture with a right handed helix of $Q_A = 0.01$ and $Q_B = 0.005$. For a large value of the ϵ_x, the wavenumber has a maximum as a function of ϕ_A. (b) Order parameters plotted against ϕ_A.

3.2. *Helical inversions in binary cholesteric mixtures.*

In this subsection, we examine the helical pitch in binary mixtures of cholesteric LC molecules. In this case, each component has an own chirality of a right- ($Q_i > 0$) or a left-handed ($Q_i < 0$) helix. The following numerical results are shown for the binary mixtures where both chiral LC molecules have a right- (or left-) handed helix and for the mixtures of a right- and a left-handed helices. We here set $n_A = 2$, $n_B = 3$, $\epsilon_n = 0.9$, and $\epsilon_{nB} = 0.95$.

Figure 4(a) shows the pitch wavenumber Q^*/Q_A plotted against the concentration ϕ_A for various values of $\epsilon_x (= \lambda_x/Q_A)$ at $\tau = 0.92$ in the chiral mixtures with a right handed helix of $Q_A = 0.01$ and $Q_B = 0.005$ in the pure components. For a large value of the ϵ_x, the wavenumber has a maximum. As decreasing ϵ_x, the pitch wavenumber has a minimum. When $\epsilon_x = -1.0$ and -1.5, the helical inversion takes place at two concentrations. The negative values of ϵ_x means that the unlike components tend to twist in the left-handed, even if the pure component has a right-handed helix ($Q_i > 0$). Figure 4(b) shows the order parameters plotted against ϕ_A for $\epsilon_x = -1$ in Figure 4(a). The values of order parameters are almost constant: $\tilde{S} \simeq 1.2$.

When $\epsilon_n \simeq \epsilon_{nB} \sim 1$ and $\tilde{S} \sim 1$, Equation (27) can be approximately given by

$$\begin{aligned} Q^* &\simeq Q_A\phi_A^2 + 2Q_A\epsilon_x\tilde{S}\phi_A\phi_B + Q_B\phi_B^2 \\ &= Q_A\big[\Lambda + 2(\epsilon_x\tilde{S} - \Lambda)\phi_A + (1 - 2\epsilon_x\tilde{S} + \Lambda)\phi_A^2\big], \end{aligned} \tag{35}$$

where we define $\Lambda \equiv Q_B/Q_A$. When $\phi_A = 0$ ($\phi_A = 1$), we have $Q^* = Q_B$ ($Q^* = Q_A$). The helical twisting power $H_{CC}(\equiv Q^*/\phi_A)$ of the binary cholesteric mixture at dilute solutions of the chiral molecule A is given by

$$H_{CC} = 2Q_A(\epsilon_x \tilde{S} - \Lambda). \tag{36}$$

When $H_{CC} < 0$, the slope of the wavenumber versus ϕ_A is a negative value for $Q_A > 0$.

The concentration of the helical inversion ($Q^* = 0$) is given by

$$\phi_{HI} = \frac{\Lambda - \epsilon_x \tilde{S} \pm \sqrt{(\epsilon_x \tilde{S})^2 - \Lambda}}{1 - 2\epsilon_x \tilde{S} + \Lambda}, \tag{37}$$

and the maximum or minimum of the pitch wavenumber occurs at

$$\phi_m = \frac{\Lambda - \epsilon_x \tilde{S}}{1 - 2\epsilon_x \tilde{S} + \Lambda}. \tag{38}$$

The ratio of the two concentrations is given by

$$\frac{\phi_{HI}}{\phi_m} = 1 \pm \frac{\sqrt{(\epsilon_x \tilde{S})^2 - \Lambda}}{\Lambda - \epsilon_x \tilde{S}}. \tag{39}$$

In Figure 4(a), when $\Lambda = 0.5$, $\epsilon_x = -1$, and $\tilde{S} = 1.2$, we obtain $\phi_{HI} = 0.19$, 0.68, and $\phi_m = 0.43$. Due to Equation (37), the condition of the helical inversion is given by

$$(\epsilon_x \tilde{S})^2 > \Lambda. \tag{40}$$

When $(\epsilon_x \tilde{S})^2 = \Lambda$, the wavenumber has a multiple root as a function of ϕ_A at

$$\phi_{root} = \epsilon_x \tilde{S}/(\epsilon_x \tilde{S} - 1). \tag{41}$$

Using $\Lambda = 0.5$, we obtain $\phi_{root} = 0.45$ with $\epsilon_x = -0.59$ for $\tilde{S} \simeq 1.2$ in Figure 4(a). The twofold helical inversion takes place for $\epsilon_x < -0.59$.

Figure 5 shows the pitch wavenumber Q^*/Q_A plotted against the concentration ϕ_A for various values of $\epsilon_x (= \lambda_x/Q_A)$ at $\tau = 0.92$ in the binary mixtures of chiral LC molecules with a right handed helix $Q_A = 0.01$ and a left-handed $Q_B = -0.03$ in the pure components: $\Lambda = -3$. For larger (smaller) values of the ϵ_x, the wavenumber has a maximum (minimum) at ϕ_m as a function of ϕ_A. The concentration ϕ_m (Equation (38)) approaches to 0.5 as increasing ϵ_x. The helical inversion takes place for all ϵ_x at ϕ_{HI}. For example, using Equation (37), when $\epsilon_x = 0$ we obtain $\phi_{HI} \simeq 0.635$. As increasing the chirality ϵ_x, the value of ϕ_{HI} shifts to lower concentrations. These numerical calculations are consistent with the experimental results in binary cholesteric mixtures.(*14*) The chiral interaction between unlike molecules is an important parameter to describe sign of the helical pitch. It is useful to suggest that "racemic mixtures" composed by equal amounts of left- and right-handed chiral molecules correspond to the case of $Q_A = -Q_B$, or $\Lambda = -1$, and $\phi_{HI} = 0.5$. Using Equation (37), the racemic mixtures of $Q^* = 0$ correspond to $\epsilon_x = 0$.

Figure 6(a) shows the pitch wavenumber Q^* plotted against the concentration ϕ_A for various values of ϵ_x at $\tau = 0.92$ in the chiral binary mixture

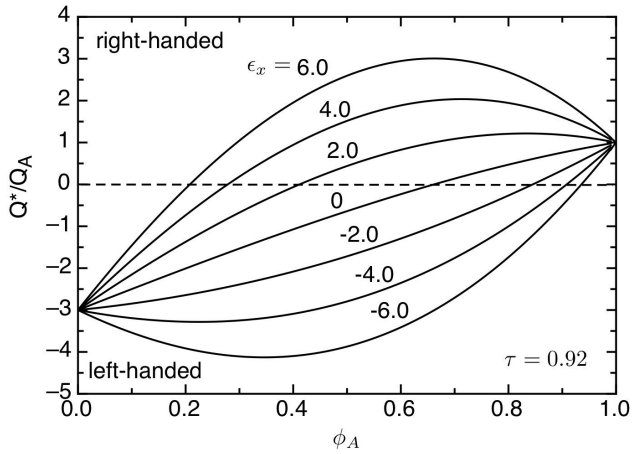

Figure 5. Pitch wavenumber Q^*/Q_A plotted against the concentration ϕ_A for various values of the chiral parameter ϵ_x at $\tau = 0.92$ in the binary cholesteric mixture with a right handed helix $Q_A = 0.01$ and a left-handed $Q_B = -0.03$ in the pure components. The helical inversion takes place at ϕ_{HI} (Equation (37)) .

with right-handed helixes in the pure components. The closed circlers show the experimental results for the binary mixture of a cholesteryl 2-(ethoxy ethoxy) ethyl carbonate (CEEC: molecule A) and an amyl-*p*-(4 cyanobenzylidene amino)-cinnamate(CBAC: molecule B). The experimental reciprocal pitches $1/p_A$ and $1/p_B$ are determined as 0.5 nm^{-1} and 1.7 nm^{-1}, respectively.(*13*) We can estimate $Q_A = 0.016$ and $Q_B = 0.053$ ($\Lambda = 3.31$) by using d_0=0.5 nm. The solid and dotted curves show the numerical results of Equation (27) and the approximate formula (Equation (35)), respectively. The wavenumber of $\epsilon_x = -6.0$ shows the good agreement with the experiments. The values of the helical inversion ϕ_{HI} and ϕ_m are given by Equations (37) and (38), respectively. As shown in Figure 6(b), the value of the order parameter $\tilde{S}$ decreases slightly with increasing ϕ_A and is almost constant $\tilde{S} \sim 1$. We then obtain $\phi_{root} = 0.64$ with $\epsilon_x = -1.8$. When $\epsilon_x < -1.8$, the twofold helical inversion takes place in the mixtures of cholesteric molecules having the same helical sense.

Some qualitative explanations for a helical inversion have been discussed by using the length of side chains.(*1, 8, 14*) Leder has discussed that the cholesteryl skeleton is effectively right-handed and the additions at the 3β-carbon of the first ring tend to reduce the right handedness.(*8*) Figure 7 shows the schematic representation of chiral molecules A (gray) and B (blue). The molecule A has a side chain A_s (yellow boxes) at the corner of the molecule A. The molecule B has a side chain B_s (red boxes) at a distance d from the corner of the molecule B. The chirality of the molecules comes from the excluded volume effects between the side-chains, including the interaction such as dipole-quadrupole interactions(*17*). As increasing d, the helix tends to reduce the right handedness. The chiral interaction between the side chains $i_s (i = A, B)$ is given by c_i. When the chiral interaction between the side chains i_s is attractive: $c_i > 0$, we have a right-handed helix of the pure molecule A (Figure 7(a)) and the pure B (Figure 7(b)). When the molecules A and B are mixed, if the interaction between the side chains A_s and B_s is attractive: $c_{AB} > 0$, the right-handed helix appears in the mixture (Figure 7(c)). Similarly, when the chiral interaction is repulsive: $c_i < 0$, we have a left-handed helix of the pure molecule A (Figure 7(d)) and the pure B (Figure 7(e)) because the side chains i_s tend to leave each others. When the molecules A and B are mixed, if the interaction between the side chains A_s and B_s is repulsive: $c_{AB} < 0$, the left-handed helix appears in the mixture (Figure 7(f)). In generally, when the chiral

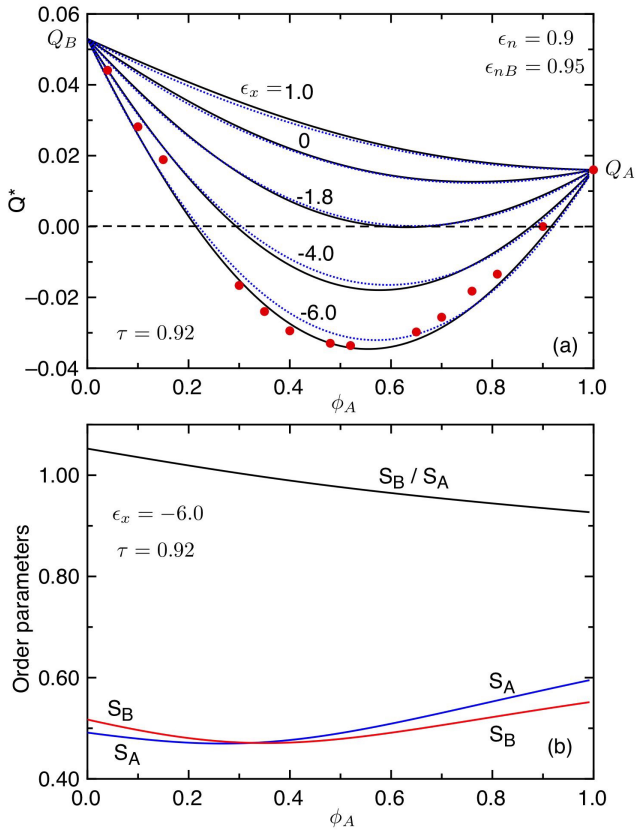

Figure 6. (a) Pitch wavenumber Q^*/Q_A plotted against the concentration ϕ_A for various values of $\epsilon_x (= \lambda_x/Q_A)$ at $\tau = 0.92$ in the binary cholesteric mixture with a right handed helix of $Q_A = 0.016$ and $Q_B = 0.053$. The solid and dotted curves show the numerical results of Equation (27) and the approximate formula (Equation (35)), respectively. The closed circlers show the experimental results.(*13*) (b) Order parameters plotted against ϕ_A.

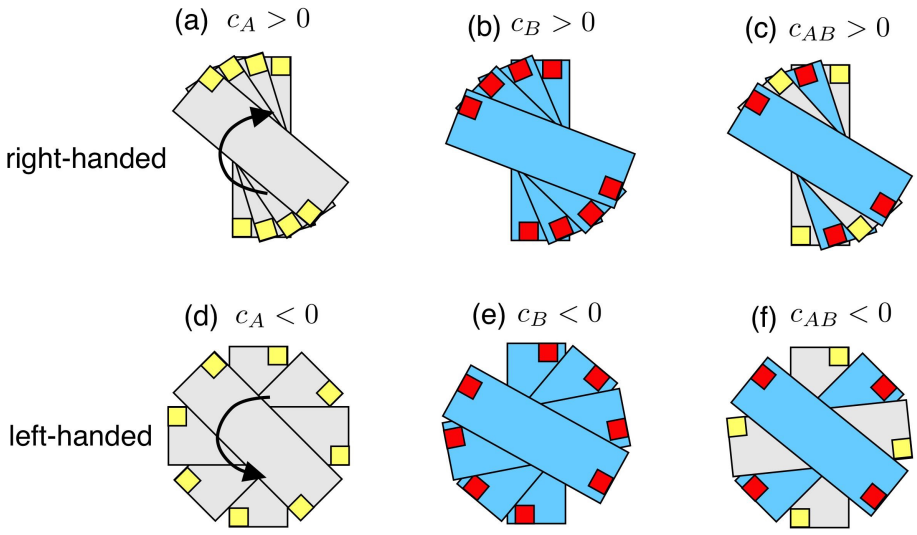

Figure 7. (Color online) The molecule A has two side chains A_s (yellow boxes) at the corners of the molecule A: (a), (d). The molecule B has two side chains B_s (red boxes) at a distance d from the corner of the molecule B: (b), (e). The chirality of the molecules comes from the excluded volume effects of the side chains i_s $(i = A, B)$. Figures (c) and (f) show the mixing of the molecules A and B: Right-handed helix (c) and left-handed helix (f) induced by two chiral molecules A and B.

interaction between the same side chains is attractive: $c_A > 0$ and $c_B > 0$, but when the chiral interaction between the unlike side chains is repulsive $c_{AB} < 0$, the left-handed helix is induced by mixing of the two chiral molecules A and B with a right-handed helix, as shown in Figure 6(a). The experiment of CEEC+CBAC mixture in Figure 6(a) may correspond to Figure 7(a) for CEEC, Figure 7(b) for CBAC, and Figure 7(f) for the mixture. These explanations are not an exact reason for the helical inversion of the experiment, however, it will help to understand the chiral interaction parameter c_{AB}, or ϵ_x and the twofold helical inversions.

3.3. *Phase separations and helical inversions in mixtures of a nematic and a cholesteric LC molecule*

In this subsection, we examine CIT and helical inversions depending on temperature and concentration in nematic-cholesteric mixtures. In Equation (2), the Flory-Huggins interaction parameter $\chi(\propto 1/T)$ shows the isotropic interaction between molecules A and B. The LC molecules A and B usually show a continuous good miscibility ($\chi = 0$) in the mixture. In general, the situation is more complex. Depending on the chemical components of the molecules, χ becomes positive values. For larger values of χ, the unlike molecules are unfavorable each other and macroscopic phase separation appears. According to the Flory-Huggins theory,(*42, 43*) the phase separations takes place at

$$\chi > \chi_c = \frac{2n_A}{(\sqrt{n_A} + \sqrt{n_B})^2}, \tag{42}$$

where χ_c is the critical point (CP). For the numerical calculations, we define the nematic interaction parameter $\alpha \equiv \nu_A/\chi$, which has been discussed in mixtures of nematic and non-nematic molecules.(*43, 46, 47*) The parameter χ is given by $\chi = \nu_A/\alpha$ and varies inversely with the temperature τ. Smaller values of α mean stronger repulsive interactions between unlike components and phase separations can take place. It has been reported a large variety of phase diagrams in binary mixtures of nematic liquid crystals.(*32, 33*) For larger values of α, the mixture shows good miscibility.

To construct the phase diagrams on the temperature-concentration plane, we calculate the free energy as a function of concentration and use the common tangent construction for finding the concentrations of coexisting phases.(*43*) We set $n_A = n_B = 2$, $\epsilon_n = 0.9$, $\epsilon_{nB} = 0.95$, and $Q_A = 0.01$.

Figure 8(a) and (b) show the dimensionless free energy $f(= f_{mix} + f_{ani})$ (Equation (1): red line) and the isotropic free energy f_{mix} (Equation (2): blue line) plotted against the concentration ϕ_A at $\tau = 0.93$ for $\alpha = 2.5$. Note that Figure 8(a) is for $\phi_A < 0.3$ and Figure 8(b) for $0.3 < \phi_A < 0.8$. The CIT takes place at ϕ^*_{CI} (a) and ϕ^{**}_{CI} (b), where the free energy of the isotropic phase and that of the Ch phase becomes equal. The dotted line in Figures 8(a) and (b) shows the common tangent construction for coexisting phases in an equilibrium state.(*43*) In Figure 8(b), the concentrations $\phi_I < \phi_A < \phi_{Ch}$ between the two tangent concentrations: ϕ_I and ϕ_{Ch}, correspond to the biphasic region, where the I and Ch^l phases coexist. At low concentrations (see Figure 8(a)), the two coexisting concentrations ϕ_I and ϕ_{Ch} approach to ϕ^*_{CI} and the biphasic region becomes narrow. The orientational order parameters jump at ϕ^*_{CI} and ϕ^{**}_{CI}, as shown in Figure 8(c). By numerically solving these concentrations of coexisting phases, we can construct the phase diagrams on the temperature-concentration plane.

Figure 9 shows the numerical results of the phase diagrams for a nematic-

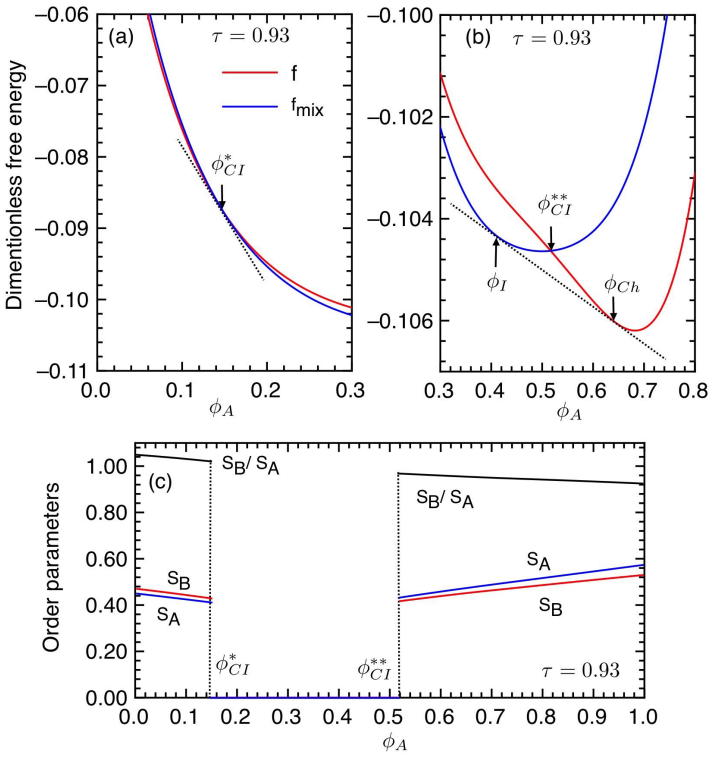

Figure 8. (Color online) Dimensionless free energy $f(= f_{mix} + f_{ani})$ (red line) and the isotropic free energy f_{mix} (blue line) plotted against the concentration ϕ_A at $\tau = 0.93$ for $\phi_A < 0.3$ (a) and $0.3 < \phi_A < 0.8$ (b) with $\alpha = 2.5$. (c) The orientational order parameters are plotted against concentration.

cholesteric mixture with $\alpha = 5$ (a), 2.7 (b), 2.5 (c), and 2.2 (d). The NIT temperature T_{NI} of the pure molecule B is given by $T_{NI}/T_{CI} = \epsilon_{nB} = 0.95$. When the nematic interaction parameter between unlike molecules A and B is $\epsilon_n = 0.9(< 1)$, the nematic interaction between the dissimilar molecules is weak relative to that in the same species and the CIT curves (broken-line) have a minimum as a function of ϕ_A. The solid curves are the binodal curves, which show the coexisting phases. Between the biphasic regions, a phase separation takes place and two phases coexist (horizontal dotted-lines). The red-lines show the helical inversion line, or the concentration ϕ_{HI}, at which the helical inversion takes place for $\epsilon_x = -1.0$ (See Figure 1). The left (right) side of this red-line corresponds to the left- (right-)handed helix. In Figure 9(a), the phase separation $(I + Ch^r)$ between the isotropic and Ch^r phase with a right-handed helix appears at $\phi_A > \phi_{HI}$. That means the domain of a Ch^r phase with a right-handed helix appears in the isotropic matrix. When $\phi_A < \phi_{HI}$, we have the phase separation $(I + Ch^l)$ between the isotropic and Ch^l phase with a left-handed helix. The concentration difference between the coexisting phases is small as shown in Figure 8(a) and the mixture has a good solubility, which corresponds to usual nematogens mixtures. At low temperatures, the stable Ch^l and Ch^r phases appear for all concentrations. In Figure 9(b) of $\alpha = 2.7$, below the Ch phase, the phase separation $(Ch^l + Ch^l)$ between two Ch phases with left-handed helix appears .The closed-circle shows the CP.

As decreasing α, the unfavorable interaction χ between unlike molecules becomes strong and the CP shifts to higher temperatures. In Figure 9(c), the binodal curve cross the helical inversion line at $\phi_A \simeq 0.7$. At lower temperatures of $\tau < 0.9$, we have the phase separation $(Ch^l + Ch^r)$ between the Ch^l phase with a left-handed helix and the Ch^r phase with a right-handed helix. At $\tau \simeq 0.92$, the biphasic region exists lower concentrations than ϕ_{HI} and then we have the phase

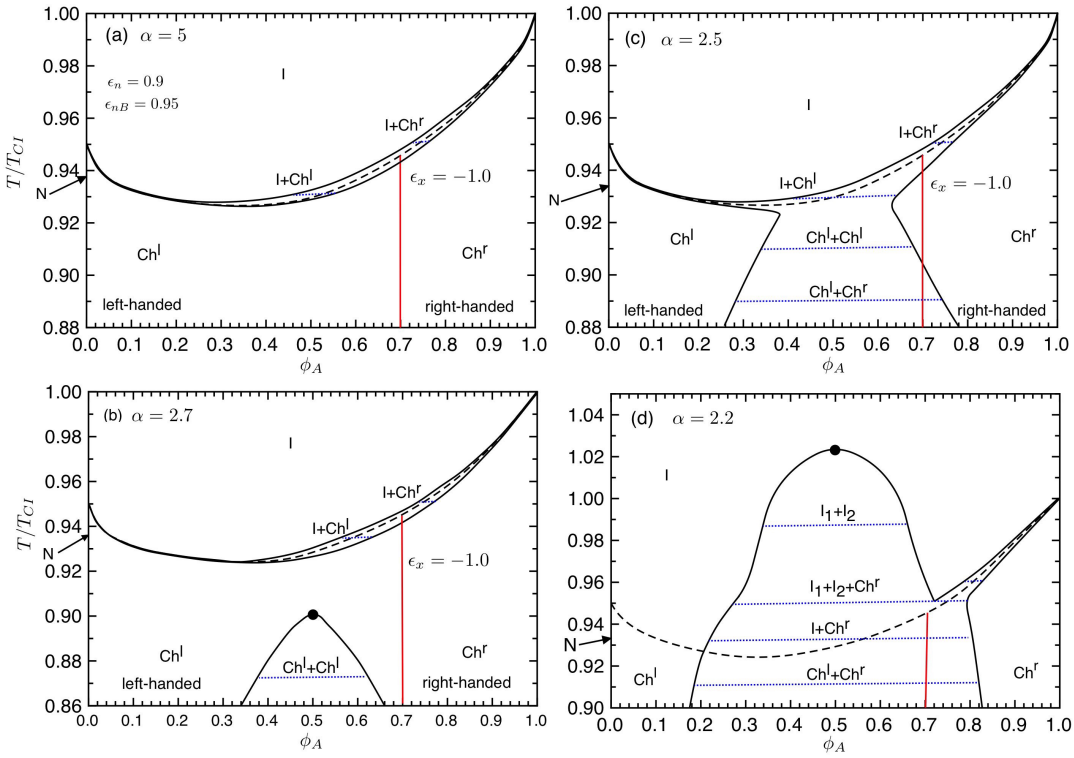

Figure 9. (Color online) Phase diagrams of nematic-cholesteric mixtures on the temperature-concentration plane with $\alpha = 5$ (a), 2.7 (b), 2.5 (c), and 2.2 (d). We set $n_A = n_B = 2$, $\epsilon_n = 0.9$, $\epsilon_{nB} = 0.95$. The broken-line shows the CIT curve. The solid lines correspond to the coexisting phases, or binodal curves. Between the binodal curves, a phase separation takes place and two phases coexist (dotted-lines). The red-line (helical inversion line) shows the concentration ϕ_{HI} at which the helical inversion takes place for $\epsilon_x = -1.0$ (See Figure 1).

separations $Ch^l + Ch^l$. As increasing temperatures, the $I + Ch^l$ phase separation appears. Figure 8(a) and (b) show the free energy at $\tau = 0.93$. Further decreasing the value of α (Figure 9(d)), the CP shifts to higher temperatures and the phase separation $(I_1 + I_2)$ between two isotropic phases with the CP appears. We also have three phase coexistence $(I_1 + I_2 + Ch^r)$ at $\tau \simeq 0.95$, where two isotropic phases and the Ch^r phase with the right-handed helix coexist. At low temperatures, the helical inversion line exists inside the coexisting curves. Then, below the triple point $(\tau < 0.95)$, the phase separations $I + Ch^r$ and $Ch^l + Ch^r$ appear. In Figure 9, we have focused on $\epsilon_x = -1$. As shown in Figure 1, the concentration ϕ_{HI} decreases with increasing ϵ_x. Depending on the value of $\epsilon_x (< 0)$, we can expect a rich variety of phase separations including the helix inversions.

4. Summary

We present a mean field theory to describe helical inversions in nematic-cholesteric mixtures and binary mixtures of cholesteric LC molecules. Taking into account the chiral coupling $\epsilon_x (\equiv c_{AB}/c_A)$ between unlike components in the mixtures, we derive the helical pitch as a function of orientational order parameters and concentration (Equations (27), (30), and (35)). The concentration ϕ_{HI} of the helical inversion and ϕ_m, at which the wavenumber has a maximum or minimum, are derived as a function of the chiral interaction ϵ_x and the orientational order parameters. In nematic and cholesteric mixtures, the condition of the helical inversion is given by $\epsilon_x \tilde{S} < 0$ (Equations (32)-(34)). In cholesteric mixtures, it is given by $(\epsilon_x \tilde{S})^2 > \Lambda$

(Equations (37)-(40)). Our theory has a good agreement with the experimental results.

The relations between the CIT and the helical inversions are also examined. Various phase separations such as $I + Ch^r$, $I + Ch^l$, and $Ch^l + Ch^r$ are predicted on the temperature-concentration plane. The concentration ϕ_{HI} of the helical inversion and the CIT concentration ϕ_{CI} are important to describe the phase diagrams. These phase diagrams including the CIT and the helical inversion have not been observed yet, however, it will be a challenging subject for chiral mixtures. Our theory demonstrates that there are a rich variety of phase separations in nematic-cholesteric mixtures and binary cholesteric mixtures, depending on the helix sense.

Finally, it is interesting to understand our results compared to Ref. (*28*). Emelyanenko, Osipov, and Dunmur have theoretically studied the helical inversion in mixtures of nematic and cholesteric mixtures by taking into account molecular biaxiality of chiral molecules. Using the orientational order parameter S_i for the nematic ordering of the long molecular axes and the order parameter D, which is not considered in our theory, of the short molecular axes of biaxial molecules in a uniaxial nematic phase, the wavenumber is derived as a function of the order parameters (S_i and D) and concentration. When we neglect the order parameter D, the wavenumber obtained by Emelyanenko et.al. results in Equation (30). The chiral interaction parameter $\epsilon_x (\equiv c_{AB}/c_A)$ can be written by $\epsilon_x = J^{212}_{1(NC)}/J^{212}_{1(CC)}$ in their notations. Using the standard Gay-Berne potential, the chiral (pseudoscalar) coupling constant $J^{212}_{1(NC)}$ between nematic and chiral molecules and the $J^{212}_{1(CC)}$ between chiral molecules have been calculated as a function of the phase φ, which determines the turn of the central site of the chiral molecules with respect to a short molecular axis and specifies the particular structure of the chiral molecules. It has been shown that the value of $J^{212}_{1(NC)}$ is always negative as a function of the parameter φ, but the value of $J^{212}_{1(CC)}$ changes sign from positive to negative values at $\varphi \simeq 0.5$ as increasing the model parameter φ. Then, when $0 < \varphi < 0.5$, the chiral parameter ϵ_x becomes negative values and the helical inversion takes place. This is consistent with the condition (Equation (33)) of the helical inversion. The molecular biaxiality becomes important for $0.5 < \varphi < 0.8$.(*28*) For larger values of the model parameter φ, the helical inversion disappears because of $\epsilon_x > 0$. Our theory does not consider molecular biaxiality, however, our results demonstrate that the chiral interaction between unlike molecules is important to understand helical sense inversions. The condition (Equation (40)) of the helical inversion in binary chiral mixtures has not been solved in terms of molecular biaxiality, yet.

References

(1) Hanson H, Dekker AJ, van der Woude F. Composition and temperature dependence of the pitch in cholesteric binary mixtures. Mol Cryst Liq Cryst. 1977; 42: 15-32.
(2) Chilaya GS, Lisetski LN. Cholesteric liquid crystals: Physical properties and molecular-statistical theories. Mol Cryst Liq Cryst. 1986; 140: 243-286.
(3) Chilaya GS, Lisetski LN. Helical twist in cholesteric mesophases. Sov Phys Usp. 1981; 24: 496-510.
(4) Katsonis N, Lacaze E, Ferrarini A. Controlling chirality with helix inversion in cholesteric liquid crystals. J Mater Chem. 2012; 22: 7088-7097.
(5) Friedel G. Ann. The mesomorphic states of matter. Phys. (Paris) 1922; 18: 273-274.
(6) Adams J, Haas W, Wysocki J. Dependence of pitch on composition in cholesteric liquid crystals. Phys Rev Lett. 1969; 22: 92-94.
(7) Baessler H, Labes MM. Helical twisting power of steroidal solutes in cholesteric mesophases. J Chem Phys. 1970; 52: 631-637.
(8) Leder LB. Rotatory sense and pitch of cholesteric liquid crystals. J Chem Phys. 1971; 55: 2649-2657.
(9) Ranganath GS, Chandrasekhar S, Kini UD, Suresh KA, Ramaseshan S. Optical properties of mixtures of right- and left-handed cholesteric liquid crystals. Chem Phys Lett. 1973; 19: 556-560.
(10) Saeva FD. Wysocki JJ . Induced circular dichroism in cholesteric liquid crystals. J Am Chem Soc. 1971; 93: 5928-5929.

(11) Nakagiri T, Kodama H, Kobayashi KK. Helical twisting power in mixtures of nematic and cholesteric liquid crystals. Phys. Rev Lett. 1971; 27: 564-567.
(12) Finkelmann H, Stegemeyer H. Helixinversion in einen binäten mischsystem nematisch/cholesterisch. Naturforsch. Z. 1973; 28a: 799-800.
(13) Finkelmann H, Stegemeyer H. Doppelte helixinversion in einem binaren system cholesteriseher komponenten mit rechtshelix. Naturforsch. Z. 1973; 28a: 1046-1047.
(14) Kozawaguchi H, Wada M. Helical twisting power in cholesteric liquid crystal mixtures. I. Experimental results. J J Appl Phys. 1975; 14: 651-655.
(15) Tsukamoto M, Ohtsuka T, Morimoto K, Murakami Y. Pitch and sense of helix in mixtures of optically active azo or azoxy compounds and nematic liquid crystal. J J Appl Phys. 1975; 14: 1307-1312.
(16) Korte EH. Infrared rotatory dispersion of binary cholesteric mixtures. J Chem Phys. 1977; 66: 99-103.
(17) Goossens WJA. A Molecular Theory of the cholesteric phase and of the twisting power of optically active molecules in a nematic liquid crystal. Mol Cryst Liq Cryst. 1970; 12: 237-244.
(18) Hanson H, Dekker AJ, van der Woude F. Analysis of the pitch in binary cholesteric liquid crystal mixtures. J Chem Phys. 1975; 62: 1941-1946.
(19) Adams J, Haas W. Pitch dependence on composition in mixtures of liquid crystals. Mol Cryst Liq Cryst. 1975; 30: 1-9.
(20) Wulf A. Helical pitch in mixtures of cholesteric liquid crystals. J Chem Phys. 1974; 60: 3994-3998.
(21) Stegemeyer H, Finkelmann H. Treatment of cholesteric liquid crystalline mixtures by means of the Goossens theory. Chem Phys Lett. 1973; 23: 227-232.
(22) van der Meer BW, Vertogen G. The helix inversion in cholesteric-nematic mixtures. Phys Lett A. 1979; 74: 242-244.
(23) Lin-Liu YR, Shih YM, Woo CW, Tan HT. Molecular model for cholesteric liquid crystals. Phys Rev A. 1976; 14: 445-.
(24) Lin-Liu YR, Shih YM, Woo CW. Molecular theory of cholesteric liquid crystals and cholesteric mixtures. Phys Rev A. 1977; 15: 2550-.
(25) Kimura H, Hoshino M, Nakano H. Temperature dependent pitch in cholesteric phase. J de Phys Coll. 1979; 40: C3-174-177.
(26) Dierking I, Giebelmann F, Zugenmaier P, Mohr K, Zaschke H. The origin of the helical twist inversion in single component cholesteric liquid crystals. Naturforsch. Z. 1994; 49a: 1081-1086.
(27) Varichon L, ten Bosch A, Sixou P. Composition and temperature dependence of the pitch in cholesteric binary mixtures. Liq Cryst. 1991; 9: 701-709.
(28) Emelyanenko AV, Osipov MA, Dunmur DA. Molecular theory of helical inversions in chiral nematic liquid crystals. Phys Rev E. 2000; 62: 2340-2352.
(29) Ferrarini A, Moro GJ, Nordio PL. Shape model for ordering properties of molecular dopants inducing chiral mesophases. Mol Phys. 1996; 87: 485-499.
(30) Harris AB, Kamien RD, Lubensky TC. Microscopic Origin of Cholesteric Pitch. Phys Rev Lett. 1997; 78: 1476-1479.
(31) Harris AB, Kamien RD, Lubensky TC. Molecular chirality and chiral parameters. Rev Mod Phys. 1999; 71: 1745-1757.
(32) Brochard F, Jouffroy J, Levinson P. Phase diagrams of mesomorphic mixtures. J Phys France. 1984; 45: 1125-1136.
(33) De Gennes PG, Prost J. The physics of liquid crystals. New York (NY): Oxford University Press; 1993
(34) Chandel VS, Singh AK, Manohar S, Shukla JP, Manohar R. Phase transition study of binary mixture of cholesteric liquid crystals. J Adv Res Phys. 2012; 3: 021203.
(35) Griffen CW, Porter R. Phase studies on binary systems of cholesteric ester A. Two aliphatic ester pairs. Mol Cryst Liq Cryst. 1973; 21: 77-98.
(36) Griffen CW, Porter R. Phase studies on binary systems of cholesteric ester B. Three C_{18} ester pairs. Mol Cryst Liq Cryst. 1973; 21: 99-124.
(37) Chiu HW, Kyu T. Equilibrium phase behavior of nematic mixtures. J Chem Phys. 1995; 103: 7471-7481.
(38) Matsuyama A. Theory of polymer-dispersed cholesteric liquid crystals. J Chem Phys. 2013: 139; 174906.
(39) Matsuyama A. Biaxiality of cholesteric phases in rod-like polymer solutions. Liq Cryst. 2015; 42: 423-429.
(40) Matsuyama A, Director-pitch coupling-induced twist-bend nematic phase. J Phys Soc Jpn. 2016; 85: 114606.
(41) Matsuyama A. Twist-bend nematic phases in binary mixtures of banana-shaped liquid crystalline molecules. Liq. Cryst. On line (2017).
(42) Flory PJ. Principles of polymer chemistry. Ithaca: Cornell University; 1953.
(43) Matsuyama A. Thermodynamics of flexible and rigid rod polymer blends. In: Isayev AI, editor. Encyclopedia of polymer blends. Vol. 1. Weinheim (Germany): WILEY-VCH; 2010. Chapter 2.
(44) Onsager L. The effects of shape on the interaction of colloidal particles. Ann NY Acad Sci. 1949; 51: 627-659.
(45) Maier W, Saupe A. Eine einfache molekular-statische theorie der nematischen kristallinflussigen phase. Teil I. Z Naturforsch. 1959; 14a: 882-889.
(46) Matsuyama A, Kato T. Phase separations and orientational order of polymers in liquid crystal solvents. Phys Rev E. 1999; 59: 763-770.
(47) Matsuyama A, Kato T. Phase diagrams of polymer dispersed liquid crystals. J Chem Phys. 1998; 108: 2067-2072.